

# Characterizing intra-tumoral heterogeneity of *CCNE1* amplification in ovarian cancer using digital pathology

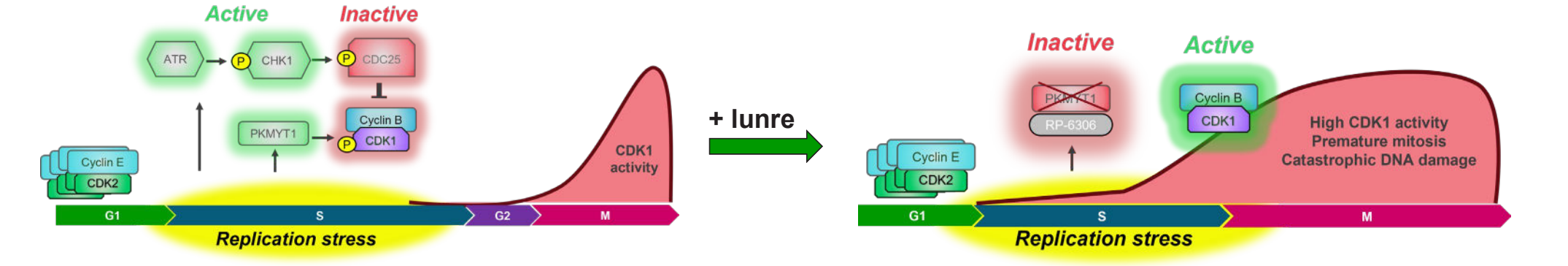
Adam Petrone<sup>1</sup>, Isabel Soria-Bretones<sup>2</sup>, Adrienne Johnson<sup>1</sup>, Sunantha Sethuraman<sup>1</sup>, Ian M. Silverman<sup>1</sup>, Jorge Reis-Filho<sup>3</sup>, Gary Marshall<sup>1</sup>, Artur Veloso<sup>1</sup>, Elia Aguado-Fraile<sup>1</sup>, Victoria Rimkunas<sup>1</sup>

<sup>1</sup>Repare Therapeutics, Cambridge, MA, USA; <sup>2</sup>Repare Therapeutics, St-Laurent, QC, Canada; <sup>3</sup>Medical Oncology, Memorial Sloan Kettering Cancer Center, New York, NY, USA



## Introduction

*CCNE1* is a gene that encodes cyclin E1 and is responsible for promoting entry and progression into S phase in tandem with CDK2<sup>1</sup>. *CCNE1* amplification is a recurrent genetic alteration that has been associated with chemoresistance and poor prognosis in gynecological malignancies. Specifically, in ovarian and endometrial cancers, *CCNE1* amplification is linked to platinum resistance and poor outcomes, representing a critical area of unmet clinical need<sup>2,3,4</sup>. Recent advances in the field of synthetic lethality have identified Protein Kinase Membrane-associated Tyrosine/Threonine 1 (PKMYT1) as synthetically lethal in tumors harboring *CCNE1* amplifications. Increased cyclin E1 pushes tumor cells into S phase which drives replication stress, requiring PKMYT1 to postpone entry into mitosis. Inhibition of PKMYT1 in *CCNE1* amplified cells causes premature mitotic entry, mitotic catastrophe and, in turn, cell death<sup>5</sup>. Lunresertib (RP-6306) is a first-in-class, highly potent and selective PKMYT1 inhibitor currently being tested in clinical trials as a single agent and in combination with the ATR inhibitor camonsertib (RP-3500), the Wee1 inhibitor Debio0123 (NCT04855656) or irinotecan (NCT05147350) in solid tumors harboring *CCNE1* amplification. A deep understanding of *CCNE1* amplification as a predictive biomarker for PKMYT1 inhibition is critical for refining patient selection strategies and strengthening our understanding of the mechanism of action. These learnings will be applied to correlative biomarker analyses in clinical trials evaluating lunre.



## Study Objective

To assess the intra-tumoral heterogeneity of *CCNE1* copy number in ovarian cancers utilizing a novel digital pathology algorithm

## Methods

**A** (n = 29) samples without *CCNE1* amp (n = 3) samples exhausted (n = 1) sample exhausted

FISH and Manual Enumeration (n = 54) ovarian serous carcinoma tumor samples → FISH and Digital Pathology Enumeration (n = 22) *CCNE1* Amp samples → Targeted NGS panel (SNIpDx) (n = 21) *CCNE1* Amp samples → Whole Genome Sequencing (WGS) and amplicon analysis (n = 8)

**B**

**FISH staining and manual enumeration**

(n = 54) ovarian serous carcinoma tumor samples

Custom *CCNE1* FISH assay

Chr19 subtelomeric control probe optimized for ploidy assessment in gyn malignancies

Manual foci enumeration

- Identification of ROIs with high target signal
- Foci enumeration (n = 50) cells

**Digital pathology**

Transfer of pathologist tissue annotations

Nuclear segmentation algorithm

- Trained: 2,609 nuclei + 178 background
- Resolution: 0.15 px
- No limits on nuclear size

Image analysis (foci quantification)

- Tissue classifier eliminated areas of oversaturation/indeterminate morphology
- Optimized FISH analysis module (IA Module v3.2.3 Halo, Indica labs)

**Data analysis pipeline**

Elimination of quantification artifacts

Nuclear size, Nuclear roundness, Chr19 Ploidy

*CCNE1* copy number spatial distribution analysis

- Single cell data used to reconstruct analyzed tissue.
- Two-dimensional histograms allow for spatial visualization of *CCNE1* CN

**Figure 1:** (A) Summary of study design and samples included per analysis. (B) Overview of FISH assay and digital pathology algorithm development. A total of 54 ovarian serous carcinoma tumor samples from the Repare biobank were analyzed for *CCNE1* copy number using a custom Fluorescence In Situ Hybridization (FISH) assay with manual foci enumeration (left panel). A custom digital pathology algorithm was developed to quantify *CCNE1*/Chr19 foci in individual cells across whole tissue slides (middle panel). An analysis pipeline was established to remove artifacts based on nuclei size, roundness, and artificial staining. Genomic data were obtained using SNIpDx Next-Generation Sequencing (NGS) panel on n = 21 *CCNE1* amplified samples. To further elucidate the genetic landscape and heterogeneity within the tumors, WGS and amplicon structural analyses (AmpliconArchitect) were performed on n = 8 samples.

## Results

### High agreement rate between manual and digital *CCNE1* FISH enumeration

Digital FISH enumeration**	<i>CCNE1</i> amplification call agreement rate	
	Manual pathology FISH enumeration *	SNIpDx Targeted NGS panel#
	18/22 (82%)	17/21 (81%)##

\* Amplification defined as mean *CCNE1*/Chr19 ratio ≥2 across n=20-50 tumor cells  
 \*\* Amplification defined as mean *CCNE1*/Chr19 ratio ≥2 across all tumor cells double positive for FITC and TRITC signal  
 # Low amplification (gain) defined as *CCNE1* copy number (CN) - tumor ploidy ≥2. Amplification defined as *CCNE1* CN + tumor ploidy ≥4  
 ## Twenty-one samples evaluated by SNIpDx, including 14 amplifications, 5 gains and 2 neutral calls

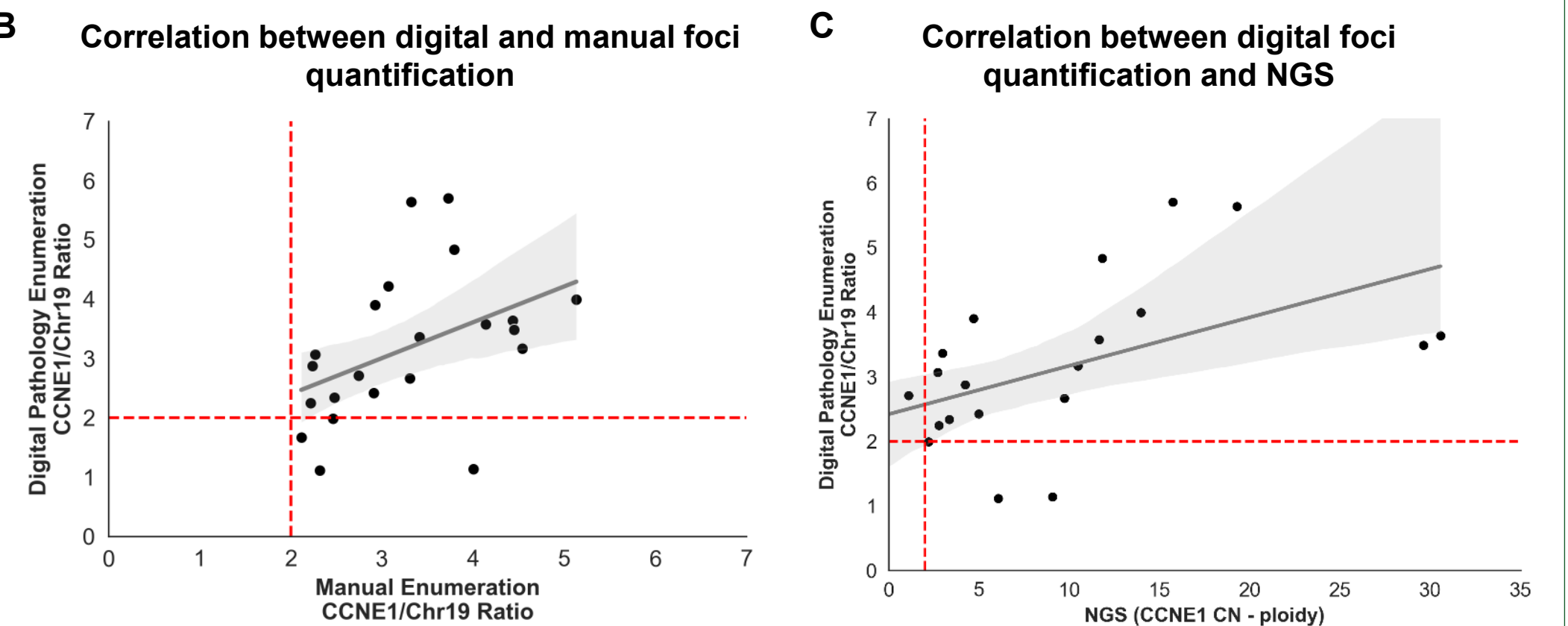


**Figure 2:** (A) *CCNE1* amplification calls were concordant in 82% samples analyzed by manual and digital FISH enumeration. Similar agreement rate (81%) was found with digital pathology and targeted NGS panel. (B) Correlation between mean *CCNE1*/Chr19 ratio values obtained by digital pathology and manual foci enumeration for each tumor specimen (Spearman  $\rho$  0.564;  $p=0.006$ ). Red dashed lines represent *CCNE1*/Chr19 ratio=2. Upper right quadrant showcases samples with concordant calls between both methods. (C) Correlation between mean *CCNE1*/Chr19 ratio obtained by digital pathology and *CCNE1* copy number over ploidy, estimated by SNIpDx (Spearman  $\rho$  0.649;  $p=0.001$ ). Horizontal red dashed line represent *CCNE1*/Chr19 ratio=2 and vertical line denotes *CCNE1* copy number (CN) - tumor ploidy=2. Upper right quadrant showcases samples with concordant amplification calls between both methods.

### Whole slide foci enumeration by digital pathology enables estimation of percentage of *CCNE1* amplified cells per tumor

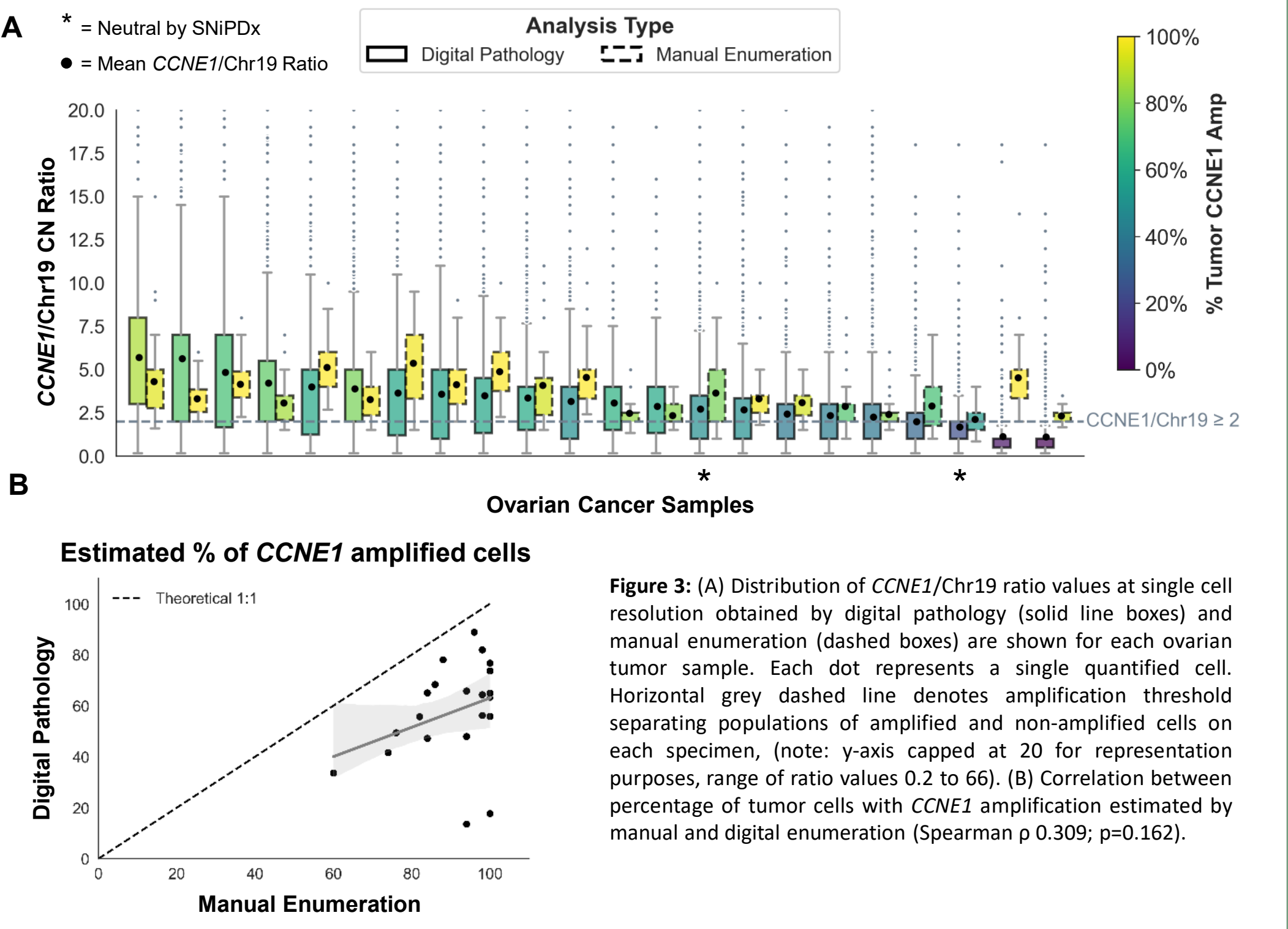
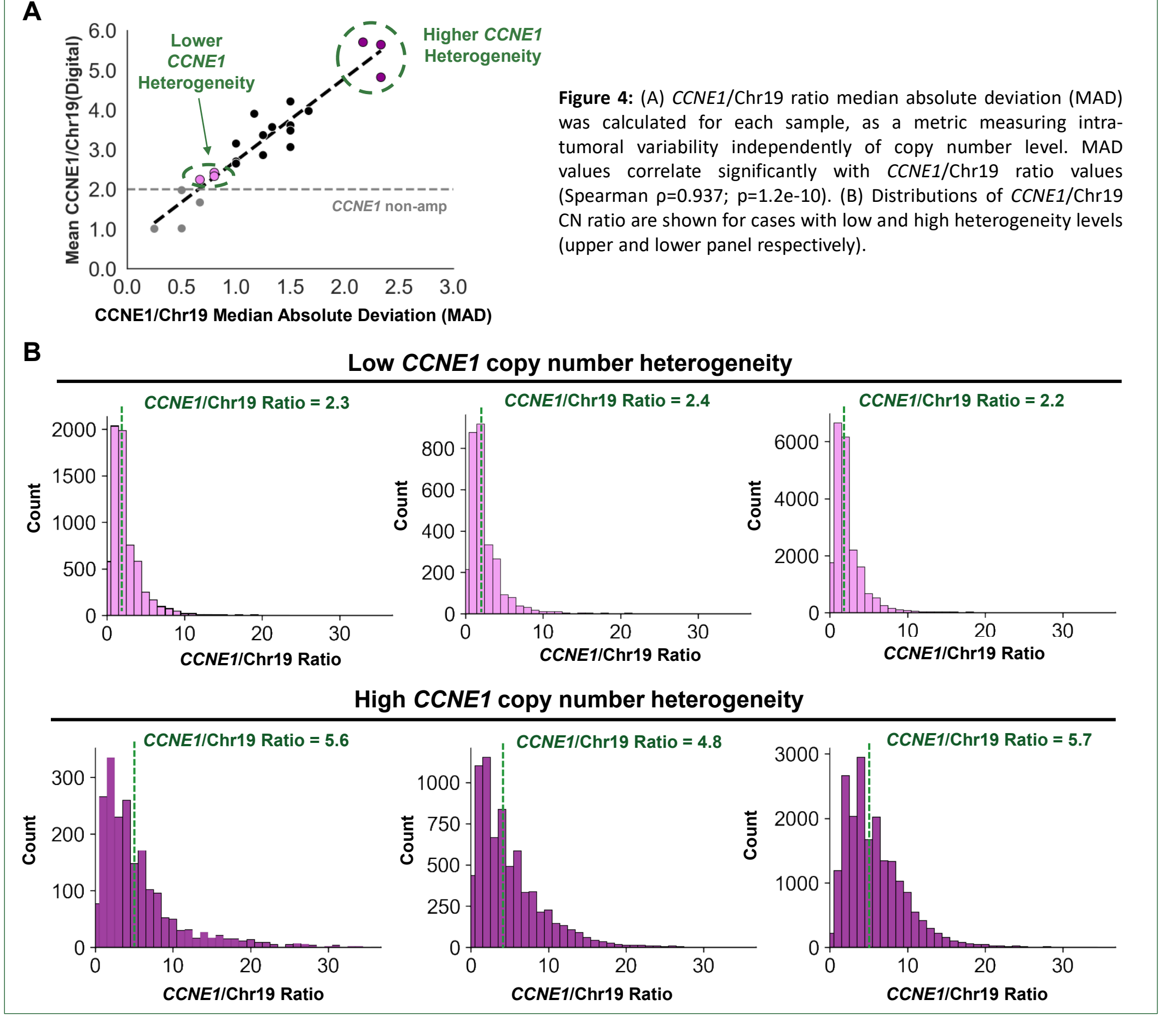


**Figure 3:** (A) Distribution of *CCNE1*/Chr19 ratio values at single cell resolution obtained by digital pathology (solid line boxes) and manual enumeration (dashed boxes) are shown for each ovarian tumor sample. Each dot represents a single quantified cell. Horizontal grey dashed line denotes amplification threshold separating populations of amplified and non-amplified cells on each specimen, (note: y-axis capped at 20 for representation purposes, range of ratio values 0.2 to 66). (B) Correlation between percentage of tumor cells with *CCNE1* amplification estimated by manual and digital enumeration (Spearman  $\rho$  0.309;  $p=0.162$ ).

## Results

### High *CCNE1* copy number amplification is associated with intra-tumoral heterogeneity



### Digital pathology enables spatial analysis of *CCNE1* copy number

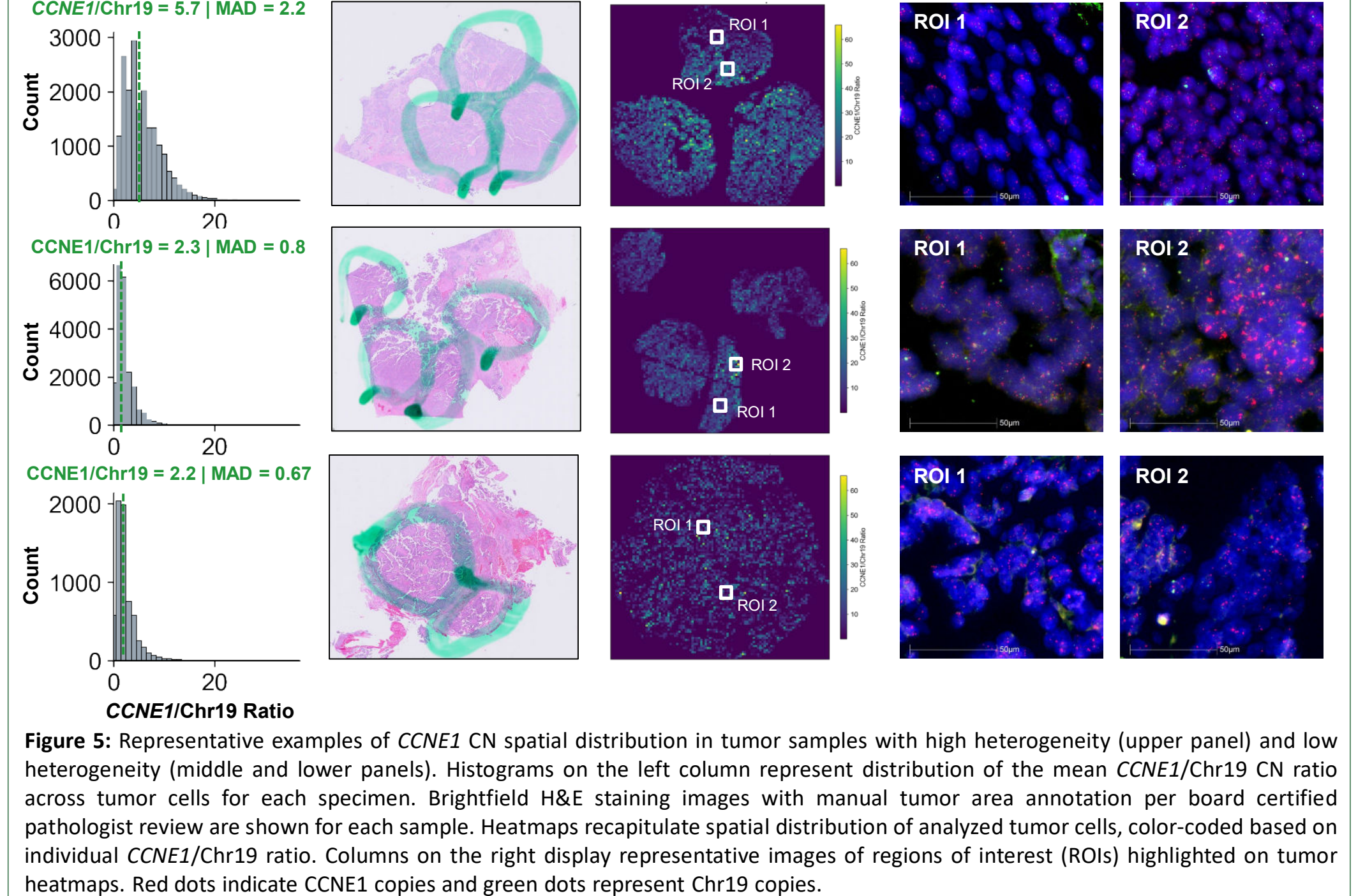


**Figure 5:** Representative examples of *CCNE1* CN spatial distribution in tumor samples with high heterogeneity (upper panel) and low heterogeneity (middle and lower panels). Histograms on the left column represent distribution of the mean *CCNE1*/Chr19 CN ratio across tumor cells for each specimen. Brightfield H&E staining images with manual tumor area annotation per board certified pathologist review are shown for each sample. Heatmaps recapitulate spatial distribution of analyzed tumor cells, color-coded based on individual *CCNE1*/Chr19 ratio. Columns on the right display representative images of regions of interest (ROIs) highlighted on tumor heatmaps. Red dots indicate *CCNE1* copies and green dots represent Chr19 copies.

## Results

### *CCNE1* CN heterogeneity may be linked to complex chromosomal rearrangements

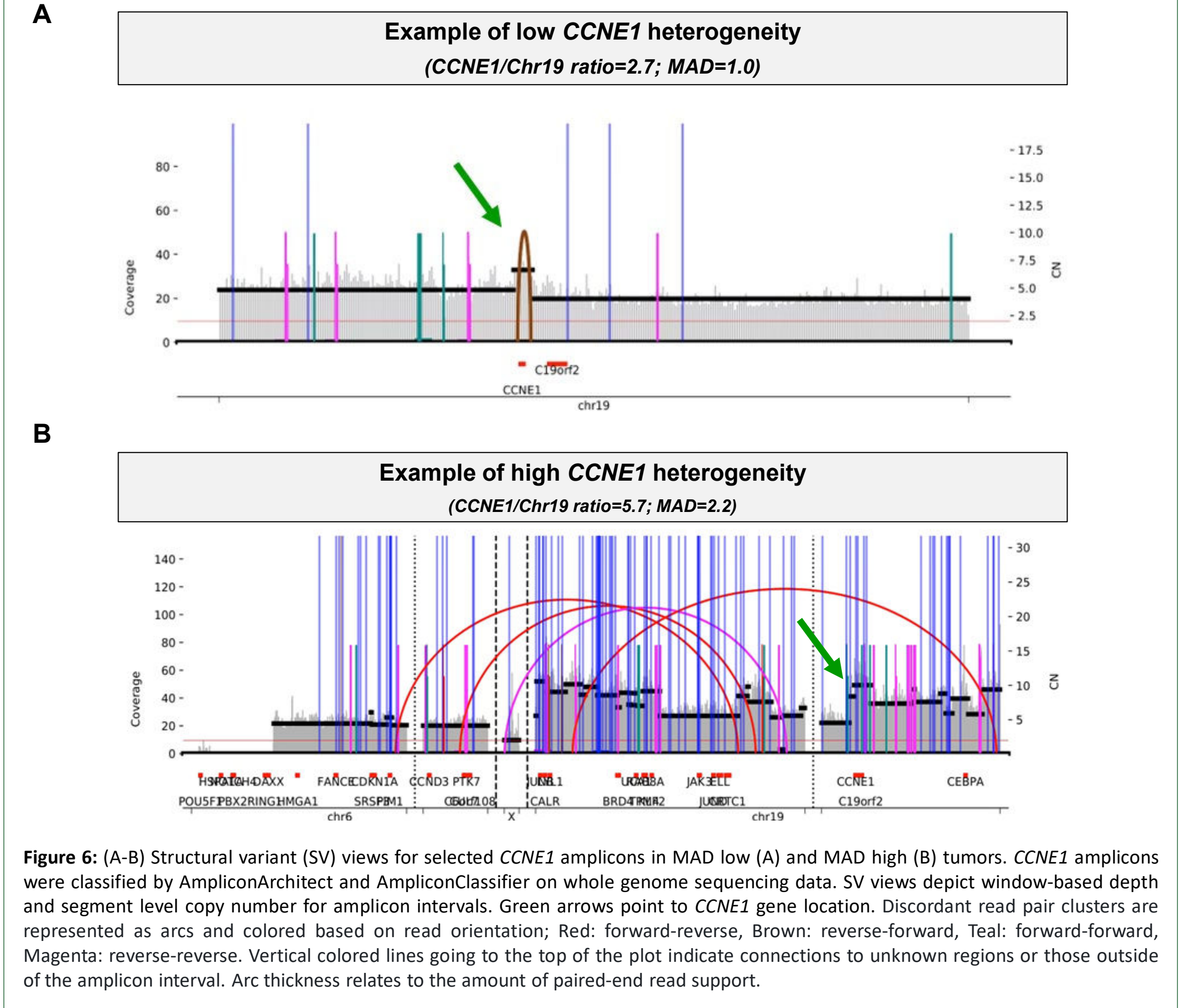


**Figure 6:** (A-B) Structural variant (SV) views for selected *CCNE1* amplicons in MAD low (A) and MAD high (B) tumors. *CCNE1* amplicons were classified by AmpliconArchitect and AmpliconClassifier on whole genome sequencing data. SV views depict window-based depth and segment level copy number for amplicon intervals. Green arrows point to *CCNE1* gene location. Discordant read pair clusters are represented as arcs and colored based on read orientation; Red: forward-reverse, Brown: reverse-forward, Teal: forward-forward, Magenta: reverse-reverse. Vertical colored lines going to the top of the plot indicate connections to unknown regions or those outside of the amplicon interval. Arc thickness relates to the amount of paired-end read support.

## Conclusions

- CCNE1* amplification is an early event in the development of ovarian cancers and is therefore expected to be homogeneously distributed in tumor cells<sup>6</sup>. However, we observed remarkable intra-tumoral heterogeneity in copy number, which is most prominent in tumors with high levels of amplification.
- Complex *CCNE1* amplicon structures accompanied by multiple chromosomal rearrangements may contribute to the observed heterogeneity in *CCNE1* copy number within a tumor.
- Future correlative biomarker studies are required to understand the clinical significance of inter- and intra-tumoral heterogeneity in *CCNE1* copy number and its relation to response to targeted therapies.
- The PKMYT1 inhibitor lunresertib demonstrates strong anti-tumor activity across a broad spectrum of *CCNE1* amplification levels in preclinical models, suggesting minimal impact from copy number heterogeneity.

## Acknowledgements/Disclosures

We would like to thank Dr. John Iafra for his contribution in the development of the customized *CCNE1* FISH assay and digital pathology algorithm used in this research. We would also like to thank Indica Labs for their support in creating the digital pathology algorithm. Finally, we would like to thank Deana Pileika and the Biomarker Operations team at Repare for handling sample management and shipment in support of this work.

J.S.R.F. is an employee of AstraZeneca and has received consultancy fees from Goldman Sachs, Paige.AI, Repare Therapeutics, and Personalis; is a member of the scientific advisory boards of Voilion Rx, Paige.AI, Repare Therapeutics, Personalis, and Bain Capital; is a member of the board of directors of Grupo Oncoclinicas; and is an ad hoc member of the scientific advisory boards of Roche Tissue Diagnostics, Ventana Medical Systems, AstraZeneca, Daiichi Sankyo, and Merck Sharp & Dohme. A.P., I.S.-B., A.J., S.J., S.M.S., G.M., A.V., E.A.-F., and V.R. are employees of Repare and may hold stock and/or stock options.

## References

- Fagundes, Rafaela, and Leonardo K. Teixeira. "Cyclin E/CDK2: DNA Replication, Replication Stress and Genomic Instability." *Frontiers in cell and developmental biology* vol. 9 774845. 24 Nov. 2021. doi:10.3389/fcell.2021.774845
- Patch, Ann-Marie et al. "Whole-genome characterization of chromosomally unstable ovarian cancer." *Nature* vol. 521 7953 (2015): 489-94. doi:10.1038/nature14419
- Eliades-Padua, Daniela et al. "Integrated genome-wide DNA copy number and expression analysis identifies distinct mechanisms of primary chemoresistance in ovarian carcinomas." *Clinical cancer research: an official journal of the American Association for Cancer Research* vol. 15 4 (2009): 1417-27. doi:10.1158/1078-0432.CCR-08-1564
- Kroger, Paul T. J., and Danny D'Orazio. "Pathogenesis and heterogeneity of ovarian cancer." *Current opinion in obstetrics & gynecology* vol. 28 1 (2017): 26-34. doi:10.1097/GCO.0000000000000340
- Gallo, David et al. "CCNE1 amplification is synthetically lethal with PKMYT1 kinase inhibition." *Nature* vol. 604 7907 (2022): 749-756. doi:10.1038/s41586-022-04638-9
- Kuhn E, Wang T, et al. "CCNE1 amplification and centrosome number abnormality in serous tubal intraepithelial carcinoma: further evidence supporting its role as a precursor of ovarian high-grade serous carcinoma. *Mod Pathol*. 2016; 29(10):1254-61. doi: 10.1038/modpathol.2016.101